

## TRANSIENT TEMPERATURE CHANGES DUE TO INCREASING CO<sub>2</sub> USING SIMPLE MODELS

by

U. Siegenthaler and H. Oeschger

(Physikalisches Institut, Universität Bern, Sidlerstrasse 5, CH-3012 Bern, Switzerland)

**ABSTRACT**

The effect of the oceanic heat capacity on global temperature response to external forcing is studied by considering a CO<sub>2</sub>-induced warming. The heat flux into the ocean is calculated using a box-diffusion model, earlier established for simulating the global carbon cycle. The calculated transient warming due to CO<sub>2</sub> produced by fossil fuel until 1980 is 0.20 to 0.26 K, or about 50% of the value for radiative equilibrium, corresponding to a delay of 16 to 24 years. Analyses of CO<sub>2</sub> in ice cores suggest a lower pre-industrial concentration, e.g. 265 ppm, than previously assumed (c. 290 ppm). The transient temperature increase until 1980 calculated for this case is about twice that for a case which starts from 297 ppm. Comparison with observations since 1880 shows that a long-term warming trend might be due to CO<sub>2</sub>, but the residual scatter unexplained by CO<sub>2</sub> is still large. Finally the different thermal behaviour of oceans and continents is accounted for in a schematic way, considering heat exchange between them. The results indicate stronger temperature variations over the continents than over the sea.

**1. GLOBAL ENERGY BALANCE**

**1.1. Basic considerations**

In the initial stages of the discussion of the CO<sub>2</sub>-climate problem the CO<sub>2</sub>-induced global warming was computed by means of climate models based on the assumption of radiative equilibrium between incoming and outgoing radiation fluxes on Earth. Recently attention has been called to the fact that the world ocean has a considerable heat capacity, and that the radiation budget is not balanced while the ocean is being heated up (Thompson and Schneider 1979, Hoffert and others 1980, Cess and Goldenberg 1981, Hansen and others 1981). We present here results of simulations of the delay and attenuation of the CO<sub>2</sub>-induced temperature change by the oceanic heat uptake, obtained using the box-diffusion model (Oeschger and others 1975) with an eddy diffusion coefficient  $K = 7\,685 \text{ m}^2 \text{ a}^{-1}$  ( $2.4 \text{ cm}^2 \text{ s}^{-1}$ ). This value has been obtained from a re-calibration of the box-diffusion model using bomb-produced <sup>14</sup>C (Siegenthaler 1983) and is larger than the value obtained using the natural <sup>14</sup>C distribution for calibration ( $4\,000 \text{ m}^2 \text{ a}^{-1}$ ). Our results are partly similar to others, although obtained independently. The general discussion will therefore be relatively short. For further details, reference is made to the cited literature, especially to Hoffert and others (1980) who used a model similar to the box-diffusion model for simulating oceanic heat transport, and who dwelt on several aspects of the problem.

Changes of the global mean surface temperature  $T$  are considered first. A global energy balance for the Earth (per m<sup>2</sup> of Earth surface) can be written as

$$\frac{d}{dt} C_E T = Q (1 - \alpha) - F \tag{1}$$

The left-hand term symbolizes changes in global heat storage with  $C_E$  representing the effective heat capacity of the Earth; it will be discussed in paragraph 1.3. On the right are the radiation fluxes at the boundary of the Earth-climate system, i.e. at the top of the atmosphere.  $Q$  is the incident solar radiation, assumed constant,  $\alpha$  is the global albedo and  $F$  denotes the outgoing infrared flux at the top of the atmosphere.

**1.2. Heat flux parameterization and equilibrium temperature changes**

Subtracting the steady-state values from Equation (1) yields the perturbation equation

$$\frac{d}{dt} C_E T = -Q \Delta\alpha - F \tag{2}$$

$Q \Delta\alpha$  denotes the effect of albedo changes on the net solar input, including variations of snow/ice cover or of cloud cover. The change of the infrared flux  $\Delta F$  can be written as

$$\Delta F = \sum_j \frac{\partial F}{\partial Y_j} \frac{dY_j}{dT} \Delta T + \frac{\partial F}{\partial \ln c} \ln(c/c_0)$$

following Watts (1980). Here,  $Y_j$  denotes all factors of influence except carbon dioxide, for instance surface temperature  $T$ , water vapour concentration or cloud cover.  $c$  is the CO<sub>2</sub> concentration,  $c_0$  its pre-industrial value. The last term takes into account the approximate variation of the infrared flux with the logarithm of the CO<sub>2</sub> concentration. Equation (2) can now be written as:

$$\frac{d}{dt} C_E T = S_C \ln(c/c_0) - S_T \Delta T \tag{3}$$

with the sensitivities

$$S_C = - \frac{\partial F}{\partial \ln c} \tag{4}$$

and

$$S_T = \sum_j \frac{\partial F}{\partial Y_j} \frac{dY_j}{dT} + Q \frac{d\alpha}{dT} \tag{5}$$

The numerical values for these sensitivities were taken from the radiative-convective model results of Augustsson and Ramanathan (1977) which include a positive water-vapour feedback process (constant relative humidity profile) and consider possible variations of cloud top altitude. They obtained, as extreme values for  $S_T$ , 2.24 W m<sup>-2</sup> K<sup>-1</sup> for constant cloud top altitude CTA and 1.38 W m<sup>-2</sup> K<sup>-1</sup> for constant cloud top temperature CTT. The CO<sub>2</sub> sensitivity of the flux appears to be relatively well established, and the value  $S_C = 6.4$  W m<sup>-2</sup> is accepted here. Once radiative equilibrium has been reached, the heat storage term in Equation (3) vanishes and the new equilibrium temperature differs from the original temperature by:

$$\Delta T_{eq} = \frac{S_C \ln(c/c_0)}{S_T} \quad (6)$$

For a CO<sub>2</sub> doubling, this yields, with the figures for  $S_C$  and  $S_T$  given above, a temperature increase of 1.98 and 3.21 K for constant CTA and constant CTT, respectively (Table I).

TABLE I. HEAT FLUX PARAMETERS AND EQUILIBRIUM TEMPERATURE CHANGES FOR CO<sub>2</sub> DOUBLING FOR THE TWO MODEL CASES (CTA: cloud top altitude, CTT: cloud top temperature)

	Constant CTA	Constant CTT
Temperature sensitivity $S_T$ (W m <sup>-2</sup> K <sup>-1</sup> )	2.24	1.38
CO <sub>2</sub> sensitivity $S_C$ (W m <sup>-2</sup> )	6.40	6.40
Equilibrium $\Delta T$ for 2 x CO <sub>2</sub> (K)	1.98	3.21

1.3. Heat storage and transport on Earth

The left-hand term of Equation (3), (d/dt)  $C_E T$ , denotes heat storage changes on Earth. It is easy to see that the main contributor to heat storage is the ocean. The atmospheric heat capacity per m<sup>2</sup> of Earth surface is  $1 \times 10^7$  J m<sup>-2</sup> K<sup>-1</sup>, that of a 100 m thick layer of ocean water is  $3.0 \times 10^8$  J m<sup>-2</sup> K<sup>-1</sup>, taking into account that the ocean covers the fraction  $f = 0.71$  of the Earth's surface. For the continent, the penetration depth of the CO<sub>2</sub>-induced warming is  $h_k = \sqrt{K_k} \tau$ , where  $K_k$  is the diffusivity of heat and  $\tau = 22.5$  a is the e-folding time of the observed CO<sub>2</sub> increase. (As long as the relative CO<sub>2</sub> excess is smaller than about 20%, the temperature response to an exponential CO<sub>2</sub> increase is also approximately exponential, and the penetration depth is  $\sqrt{K_k} \tau$ . This is found from Equation (3) when developing  $\ln(c/c_0)$ ). The effective heat capacity of the continent per m<sup>2</sup> of Earth surface, then, is  $h_k \rho C_k (1-f) = 1.2 \times 10^7$  J m<sup>-2</sup> K<sup>-1</sup> ( $h_k = 19$  m), using the values indicated by Hoffert and others (1980), i.e.  $K_k = 16$  m<sup>2</sup> a<sup>-1</sup>,  $\rho = 2800$  kg m<sup>-3</sup> and  $C_k = 750$  J kg<sup>-1</sup> K<sup>-1</sup> (specific heat). In other words, the heat capacities of the atmosphere and of the continents correspond to that of ocean layers of about 3 m and 4 m in depth, respectively, while the total penetration depth into a box-diffusive ocean with a mixed layer of 75 m and an eddy diffusivity of  $K = 4005$  m<sup>2</sup> a<sup>-1</sup> is of the order of  $75 \text{ m} + \sqrt{K} \tau = 375$  m. In the model simulation, therefore, only the oceanic heat capacity is considered.

In determining the mean global temperature change, different possibilities may be considered for taking into account the continental surface. First, we set the temperature change of the continents equal to that of the sea surface, which would correspond to a coupling coefficient  $\nu = \infty$  in Cess and Goldenberg's (1981) terminology. This implies that the continental temperature change is driven fully by the temperature

of the sea surface, or, in the one-dimensional box-diffusion model, by that of the mixed layer. In this model, the heat balance (per m<sup>2</sup> of Earth surface) for the mixed layer reads, using Equation (3):

$$f C_W \rho h_m \frac{d \Delta T_S}{dt} = S_C \ln(c/c_0) - S_T \Delta T_S + f C_W \rho K \left. \frac{\partial \Delta T_S}{\partial z} \right|_{z=0} \quad (7)$$

where  $T_S$  is the sea-surface temperature,  $f = 0.71$  is the oceanic fraction of the Earth's surface,  $h_m = 75$  m the mixed layer depth,  $C_W$  the specific heat and  $\rho$  the density of sea-water,  $K$  the eddy diffusion coefficient describing the vertical exchange rate in the deep sea (assumed to be the same for heat as for water or carbon) and

$$\left. \frac{\partial \Delta T_S}{\partial z} \right|_{z=0}$$

is the gradient of the temperature perturbation at the top of the deep-sea reservoir. The transport within the deep sea is governed by the same formulae as valid for CO<sub>2</sub>, given by Oeschger and others (1975). In contrast to the case of CO<sub>2</sub>, there is no separate heat balance equation for the atmosphere, because its heat capacity is set to zero and the global surface temperature change is, in the model, equal to the change in the mixed layer.

2. SIMULATED MEAN GLOBAL TEMPERATURE INCREASE

2.1. Step increase of forcing

The transient heat storage of the model is well characterized by considering a step increase of an external forcing mechanism, e.g. a sudden increase of atmospheric CO<sub>2</sub>.

In Figure 1 the result of the box-diffusion simulation for a stepwise CO<sub>2</sub> doubling is shown for constant CTT (cf. Table I). In the first 10 or 20 a, the temperature increases rapidly and reaches half the final value (1.6 K) after 27 a. After this initial period, however, it changes more and more sluggishly. After 100 a, the change is 69% of the equilibrium value of 3.21 K. The precise numbers depend on the values chosen for the model parameters and should not be considered as realistic. An important feature is, however, that equilibrium is not approached in an exponential way, as would be the case for a constant heat capacity. Rather the characteristic time scale, defined by  $\Delta T_{eq} (d\Delta T/dt)^{-1}$  increases with time, as does the effective heat capacity of the ocean. This reflects the characteristic behaviour of the box-diffusion model which for CO<sub>2</sub> was discussed by Siegenthaler and Oeschger (1978). The mixed layer and the upper deep-sea layers are rapidly warmed up, but it takes a very long time until the whole ocean has reached the new temperature. Until this is the case, however, heat is still transported downwards and the surface temperature is below its equilibrium value. In view of the very long time needed for reaching the equilibrium temperature, the effect of oceanic thermal inertia is not only a delay but actually also an attenuation of the temperature increase on the time scale of centuries.

2.2. Temperature response due to fossil-energy induced CO<sub>2</sub> increase

Of interest is, of course, the predicted temperature rise due to the observed CO<sub>2</sub> increase. For this purpose, this increase was simulated by means of the box-diffusion model using the CO<sub>2</sub> production data of Rotty (1983) as model input. Because here the effect of the actual CO<sub>2</sub> rise is of interest, the model was adapted so as to reproduce the observed CO<sub>2</sub> concentration (1 January 1959: 315.6 ppm, 1 January 1978: 333.8 ppm (Bacastow and Keeling 1981) by assuming a (small) additional CO<sub>2</sub> sink proportional to the

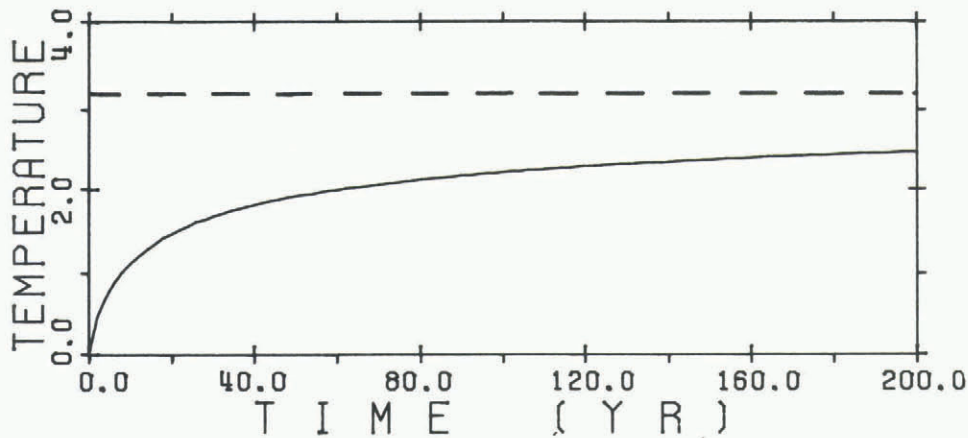


Fig.1: Transient response (solid line) of mean global surface temperature to a CO<sub>2</sub> doubling at time 0, using the box-diffusion model and assuming constant cloud top temperature (CTT). Dashed line: equilibrium response.

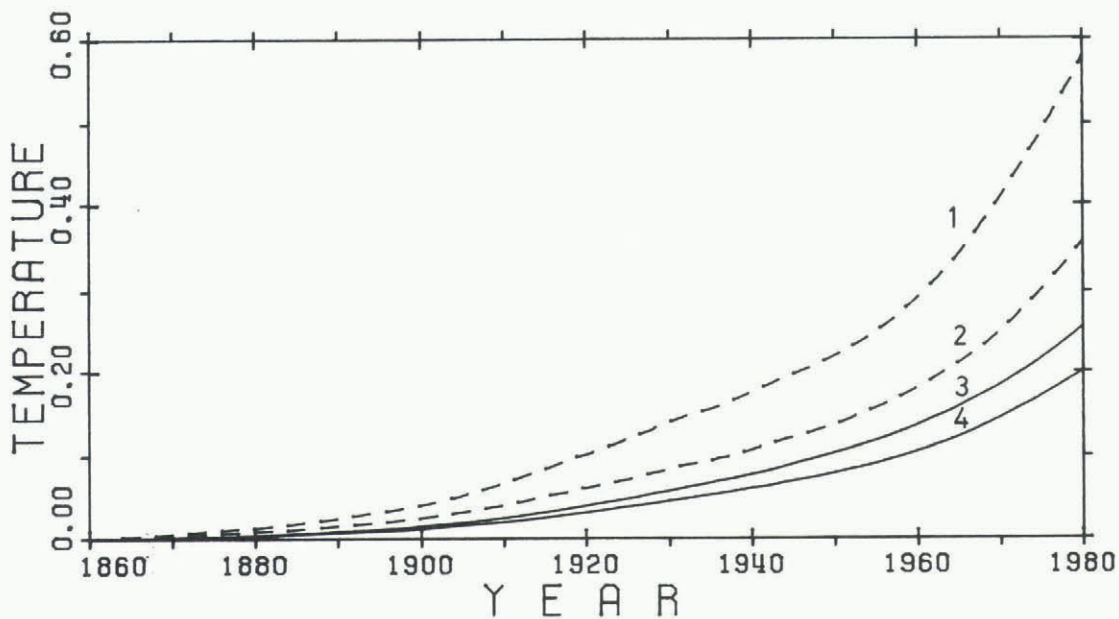


Fig.2. Transient (solid lines) and equilibrium (dashed lines) temperature response to a CO<sub>2</sub> increase starting from 297 ppm in 1860, i.e. assuming fossil input only. Curves 1, 3: constant cloud top temperature (CTT), curves 2, 4: constant cloud top altitude (CTA).

fossil production rate. The pre-industrial level (constant until 1860) was assumed to be 296.9 ppm or about 297 ppm. The results for radiative equilibrium and for the transient system are represented in Figure 2 and for 1980 in Table II(a) both for constant CTA and constant CTT. If we consider these two cases as limits, then the temperature increase computed with oceanic heat capacity is between 0.20 and 0.26K in 1980 or roughly 50% of the equilibrium value. The corresponding time delay is between 16 and 24 a. The effect of the oceanic heat capacity (attenuation by about a factor of two) is relatively strong if compared to other estimates. This is related to the method of calibration of the ocean model using bomb-produced <sup>14</sup>C, which yields a relatively large vertical diffusivity (7 685 m<sup>2</sup> a<sup>-1</sup>) and is probably more applicable to the time scales considered here than a calibration using the natural <sup>14</sup>C distribution.

### 2.3. Consequences of a low pre-industrial CO<sub>2</sub> concentration

Measurements on air bubbles occluded in old polar ice have yielded strong evidence that the pre-industrial CO<sub>2</sub> concentration was significantly lower

than the value of 290 to 295 ppm previously assumed (Oeschger and others in preparation\*). This implies that there must have been a large non-fossil input of CO<sub>2</sub> in the past, between about 50 and 150 a ago. Here we consider the consequences for the global temperature trend. For this purpose it was assumed that the concentration was 265 ppm until 1820; then it increased as a quadratic function of time to 273 ppm in 1860, rose linearly to 313 ppm in 1955 and from then on followed the same curve as assumed in the last paragraph (fossil input only). The resulting transient temperature changes are presented in Figure 3 (upper two curves) for constant CTT and CTA, together with the corresponding curves for fossil input only (lower two curves); values for 1980 are given in Table II(b). Corresponding to the

\*To be submitted for publication:

Oeschger H, Heimann M, Hofer H, Neftel A, Schwander J, Siegenthaler U, Stauffer B. Pre-industrial CO<sub>2</sub> concentration from ice cores and implications for carbon cycle and climate.

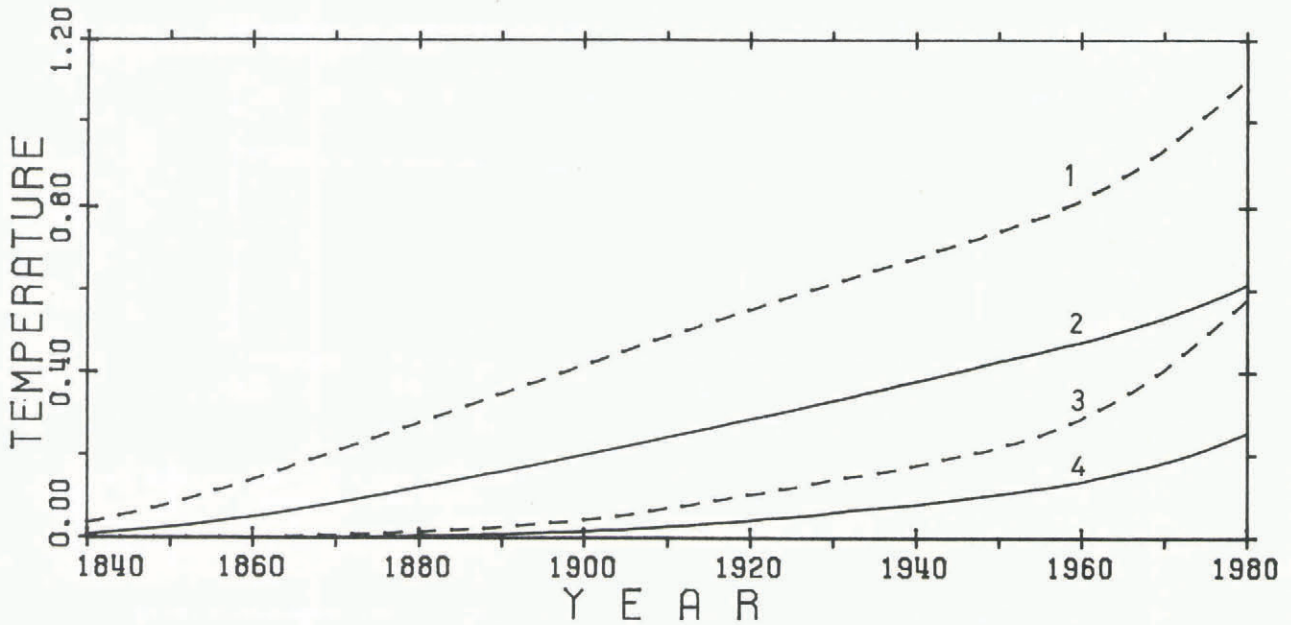


Fig.3. Transient (solid lines) and equilibrium (dashed lines) temperature responses for CO<sub>2</sub> increase starting at 297 ppm (fossil input only, curves 3, 4) and at 265 ppm (early non-fossil input, curves 1, 2). Constant CTT is assumed.

TABLE II. EQUILIBRIUM AND TRANSIENT TEMPERATURE INCREASE FOR THE CO<sub>2</sub> INCREASE UNTIL 1980, AND DELAY OF  $\Delta T$  COMPARED TO  $\Delta T_{eq}$  (CTA: V constant cloud top altitude, CTT: V constant cloud top temperature)

a) Fossil input only ( $c_0 = 297$  ppm)

	Constant CTA	Constant CTT
Equilibrium $\Delta T_{eq}$ (K)	0.36	0.58
$\Delta T$ with thermal inertia (K)	0.20	0.26
Attenuation ( $\Delta T/\Delta T_{eq}$ )	0.56	0.44
Delay (a)	16	24

b) Lower pre-industrial value ( $c_0 = 265$  ppm)

	Constant CTA	Constant CTT
Equilibrium $\Delta T_{eq}$ (K)	0.68	1.11
$\Delta T$ with thermal inertia (K)	0.46	0.62
Attenuation ( $\Delta T/\Delta T_{eq}$ )	0.69	0.56
Delay (a)	31	50

higher CO<sub>2</sub> increase until 1980 (27% of the pre-industrial value instead of 13%), the computed temperature changes are roughly twice as large as in the 297 ppm (fossil-only) case. Again the attenuation due to the oceanic heat uptake is considerable, but it is not as strong as in the 297 ppm case because the CO<sub>2</sub> has increased more slowly in the 265 ppm case, according to our assumption, than in the first case, so that the ocean has had more time to warm up.

2.4. Comparison with observed temperature trend

The observed hemispheric or global trends of surface air temperature, as compiled by different authors, exhibit considerable short-time scatter, as well as long-term trends, for instance a cooling after 1940, which cannot be explained by CO<sub>2</sub> varia-

tions alone. This is not surprising and documents that other causes, such as volcanic dust or changing insolation, influence the air temperatures. Nevertheless it is interesting to compare the observations with the computed trends due to CO<sub>2</sub>. In Figure 4, anomalies of the mean surface temperature for the northern hemisphere since 1880, as calculated by Jones and others (1982), are shown, together with model-simulated curves for pre-industrial concentrations of 265 and 297 ppm (constant CTT, transient case). Since the observed data are not for the whole Earth but for the northern hemisphere only, the model curves shown were calculated for equal ocean and continent areas ( $f = 0.5$ ), in contrast to those of Figures 1 to 3 that were obtained using  $f = 0.71$ . The model curves have been shifted so that their mean values for the period 1880-1980 are zero, as is the case for the observed anomalies. The comparison shows that the simulated curve for  $c_0 = 265$  ppm can in principle explain an observed long-term warming of about 0.5 K between 1890 and 1980 (the decade between 1880 and 1890 seems to have been unusually cold and should therefore not be given much weight). The model curve for fossil input only ( $c_0 = 297$  ppm) can explain less of the observed variations than the other model curve, in magnitude as well as in shape. In view of the large residual scatter it cannot easily be decided if this difference is significant. In order to determine whether the observed overall warming is due to CO<sub>2</sub> or not, it would be necessary to explain the residual variability. Attempts in this direction have been undertaken, invoking volcanic dust and solar variability (Hansen and others 1981), but at present the experimental data are uncertain for volcanic forcing and only speculative for solar variability.

3. FINITE ENERGY EXCHANGE BETWEEN OCEAN AND CONTINENT

3.1. Heat exchange between ocean and continent

The transport of sensible and latent heat by the atmosphere provides for a quasi-continuous energy exchange process between continents and ocean surface. In the following, we consider in a schematic way the case that this exchange flux is finite. We make the simple assumption that the exchange flux  $F_{SC}$  is proportional to the difference between the mean temperatures  $T_S$  and  $T_C$  of sea surface and continent:

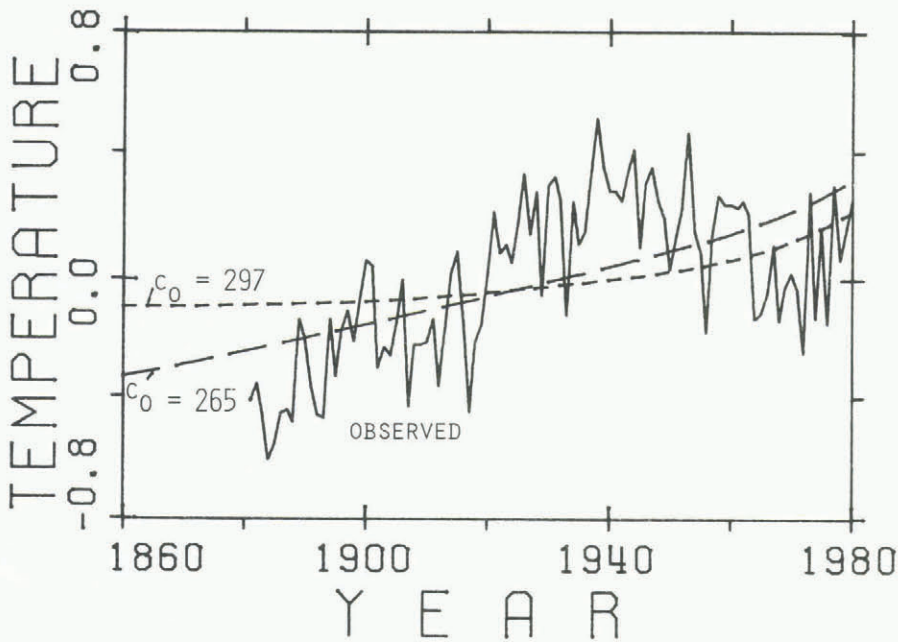


Fig.4. Observed mean northern hemisphere temperature anomalies (Jones and others 1982). Dashed lines: transient mean global temperature changes simulated for pre-industrial values of 265 and 297 ppm. Constant CTT is assumed. All three curves have been shifted so as to have a mean value of zero in the period 1880 to 1980.

$$F_{SC} = k_{SC} (T_S - T_C) \tag{8}$$

where  $k_{SC}$  is a heat transfer coefficient (units:  $W m^{-2} K^{-1}$ ). It is assumed constant, which is an over-simplification since evaporation and hence latent heat transport strongly depend on temperature, but for a first sensitivity study it may be acceptable. We assume that ocean and continent cover the same area, which approximately holds for mid-latitudes in the northern hemisphere, so that the same transfer coefficient  $k_{SC}$  (per unit area) applies for the continent and for the sea.

The heat balance for the oceanic mixed layer now is given by

$$C_W \rho h_m \frac{d \Delta T_S}{dt} = S_C \ln(c/c_0) - S_T \Delta T_S + C_W \rho K \left. \frac{\partial \Delta T_S}{\partial z} \right|_{z=0} + k_{SC} (\Delta T_C - \Delta T_S) \tag{9}$$

(cf. Equation (7)).

For the continent we have

$$0 = S_C \ln(c/c_0) - S_T \Delta T_C + k_{SC} (\Delta T_S - \Delta T_C) \tag{10}$$

Instead of the forcing by CO<sub>2</sub>, any other external perturbation of the energy balance e.g. the seasonal variation of insolation can be inserted as the first term on the right-hand side of Equations (9) and (10). This provides a means to estimate the magnitude of the transfer coefficient  $k_{SC}$ . Using as a forcing term the expression  $S_T \Delta T_0 \sin \omega t$ , with  $\omega = 2\pi a^{-1}$ , yields expressions for the seasonal temperature variations;  $\Delta T_0$  would be the temperature amplitude in the absence of any internal heat fluxes. In mid-latitudes of the northern hemisphere the ratio of the mean annual temperature amplitudes of continent and sea surface is  $4 \pm 1$ , as estimated from figure 7.20 of Wallace and Hobbs (1977). For solving the equations equivalent to (9) and (10), we take into

account only the mixed-layer heat capacity ( $h_m = 75$  m), since the seasonal variations hardly penetrate into the thermocline. Formally, this is equivalent to setting  $K = 0$  in Equation (9). With an average value of  $1.7 W m^{-2} K^{-1}$  for  $S_T$  (the exact value of  $S_T$  is not essential) we obtain

$$k_{SC} = 10.2/7.2/5.5 W m^{-2} K^{-1}$$

for continent/ocean amplitude ratios of 3/4/5, respectively. For the numerical computation, the value  $7.2 W m^{-2} K^{-1}$  has been used. An atmospheric thermal relaxation time can be calculated as  $C_a/k_{SC}$ , where  $C_a$  is an effective atmospheric heat capacity. Assuming that the layers below 500 mbar effectively contribute to the heat transport,  $C_a = 0.5 \times 10^7 W m^{-2} K^{-1}$ , and the relaxation time is eight days which appears a reasonable value.

### 3.2. Results

Transient temperature responses were computed for ocean and continent for the two CO<sub>2</sub> scenarios starting with 297 and 265 ppm, respectively. The results are plotted in Figure 5. The oceanic temperature change (solid line) is slightly smaller than the corresponding change on the continent (dashed line). The difference in 1980 is 10% for  $c_0 = 265$  ppm and 15% for  $c_0 = 297$  ppm; the relative differences would be slightly larger if constant CTA, instead of CTT had been assumed.

The simulated difference between ocean and continent is not large, but it is significant. In our model the ocean-continent heat coupling has been simulated in a very crude way, and the actual heat transfer flux may be different from the value determined here in an approximate way only (e.g. not considering the influence of ocean circulation on seasonal sea-surface temperature variations).

Although the precise result for the temperature difference ocean-continent should not be given much weight; it is large enough to warrant further inspection. Schneider and Thompson (1981) discussed the transient climatic response with respect to latitudinal differences. According to their model the approach towards equilibrium was significantly differ-

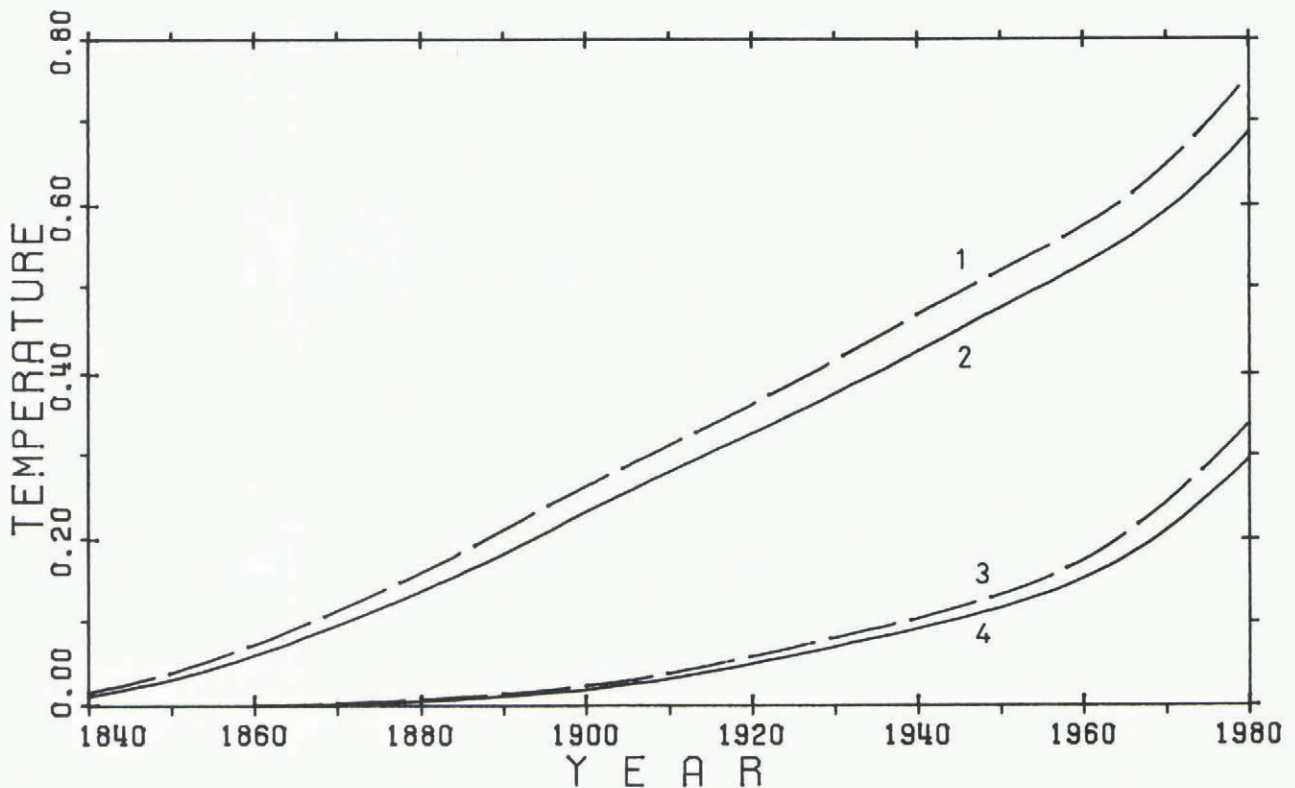


Fig.5. Transient temperature changes calculated separately for continent (dashed) and ocean (solid curves), assuming a pre-industrial value of 265 ppm (curves 1, 2) or 297 ppm (curves 3, 4).

ent in different regions, implying that the horizontal temperature gradient, and therefore the distribution of climatic change, might vary considerably from that determined, assuming equilibrium. (See also Bryan and others 1982 and Thompson and Schneider 1982 for further discussions.) This argument also applies for the distinction ocean-continent. A continuing CO<sub>2</sub> growth, mainly if it will be rapid, will imply ocean-continent differences, possibly leading to changes in atmospheric circulation.

All values (of Figure 5) are larger than those for the mean global temperature increase shown in Figure 3. The reason is that those curves were calculated with a value  $f = 0.71$  for the oceanic fraction of the Earth's surface area, while for Figure 5 (and Figure 4) equal oceanic and continental areas are assumed ( $f = 0.5$ ). The results for the mean global temperature change with  $f = 0.5$  (see Fig.4) are a few percent higher than those for the sea surface alone, as one would quantitatively expect.

#### CONCLUSIONS

- This study has yielded the following main results:
- (1) The delaying and attenuating effect of the heat capacity of the ocean is relatively large if the ocean model is calibrated based on bomb-produced <sup>14</sup>C instead of on natural <sup>14</sup>C. On time scales up to centuries, the global temperature change is significantly below its equilibrium value. Therefore the effect of the ocean's heat capacity is not just a delay of one or a few decades, as sometimes mentioned.
  - (2) If the pre-industrial CO<sub>2</sub> level  $c_0$  was about 295 ppm, the simulated warming until 1980 is only about 0.2 K. If it was, however, significantly lower, e.g. 265 ppm, then the simulated warming until 1980 may have been more than twice as large, and a good part of this warming must have taken place in the nineteenth and early twentieth centuries.
  - (3) Observed temperature trends since 1880 exhibit relatively great variation which cannot be explained

by CO<sub>2</sub>. The simulated trend with  $c_0 = 265$  ppm fits the observations slightly better than the one with  $c_0 = 297$  ppm.

(4) On the continents, the temperature changes induced by CO<sub>2</sub> or other external forcing processes are stronger than over the sea. This may imply a geographical climate response that differs from that obtained from equilibrium modelling.

#### REFERENCES

- Augustsson T, Ramanathan V 1977 A radiative convective model study of the CO<sub>2</sub> climate problem. *Journal of the Atmospheric Sciences* 34: 448-451
- Bacastow R B, Keeling C D 1981 Atmospheric carbon dioxide concentration and the observed airborne fraction. In Bolin B (ed) *SCOPE 16. Carbon cycle modelling*. New York, Wiley: 103-112
- Bryan K, Komro F G, Manabe S, Spelman M J 1982 Transient climate response to increasing atmospheric carbon dioxide. *Science* 215: 56-58
- Cess R D, Goldenberg S D 1981 The effect of ocean heat capacity upon global warming due to increasing atmospheric carbon dioxide. *Journal of Geophysical Research* 86(C1): 498-502
- Hansen J and 6 others 1981 Climate impact of increasing atmospheric carbon dioxide. *Science* 213: 957-966
- Hoffert M I, Callegari A J, Hsieh C-T 1980 The role of deep sea heat storage in the secular response to climatic forcing. *Journal of Geophysical Research* 85(C11): 6667-6679
- Jones P D, Wigley T M L, Kelly P M 1982 Variations in surface air temperatures. Part 1. Northern hemisphere, 1881-1980. *Monthly Weather Review* 110: 59-69
- Oeschger H, Siegenthaler U, Schotterer U, Gugelmann A 1975 A box diffusion model to study the carbon dioxide exchange in nature. *Tellus* 27(2): 168-192

- Rotty R M 1983 Distribution of and changes in industrial carbon dioxide production. *Journal of Geophysical Research* 88(C2): 1301-1308
- Schneider S H, Thompson S L 1981 Atmospheric CO<sub>2</sub> and climate: importance of the transient response. *Journal of Geophysical Research* 86(C4): 3135-3147
- Siegenthaler U 1983 Uptake of excess CO<sub>2</sub> by an outcrop-diffusion model of the ocean. *Journal of Geophysical Research* 88(C6): 3599-3608
- Siegenthaler U, Oeschger H 1978 Predicting future atmospheric carbon dioxide levels. *Science* 199: 388-395
- Thompson S L, Schneider S H 1979 A seasonal zonal energy balance climate model with an interactive lower layer. *Journal of Geophysical Research* 84 (C5): 2401-2414
- Thompson S L, Schneider S H 1982 Carbon dioxide and climate: the importance of realistic geography in estimating the transient temperature response. *Science* 217: 1031-1033
- Wallace J M, Hobbs P V 1977 *Atmospheric science*. New York, Academic Press
- Watts R G 1980 Climate models and CO<sub>2</sub>-induced climatic changes. *Climatic Change* 2: 387-408